

# Well-Defined Star Polymers with Mixed-Arms by Sequential Polymerization of Atom Transfer Radical Polymerization and Reverse Addition–Fragmentation Chain Transfer on a Hyperbranched Polyglycerol Core

Chao Liu, Yi Zhang, and Junlian Huang\*

The Key Laboratory of Molecular Engineering of Polymer, State Education Ministry of China, Department of Macromolecular Science, Fudan University, Shanghai 200433, China

Received June 27, 2007; Revised Manuscript Received November 13, 2007

**ABSTRACT:** Mixed-arm star polymers were synthesized by atom transfer radical polymerization (ATRP) and reverse addition–fragmentation chain transfer (RAFT) sequential polymerization using the “core first” method. The synthesis consisted of three steps: (i) synthesis of a hyperbranched polyglycerol (HPG) core, (ii) ATRP with the first monomer (St, styrene), and (iii) then the polymerization with the second monomer (*tert*-butyl acrylate, tBA) from the core by the RAFT technique. After the hydrolysis of poly(tBA), poly(acrylic acid) (PAA) arms were obtained. In the whole process, the final products and intermediates were characterized by gel permeation chromatography (GPC), nuclear magnetic resonance spectroscopy (NMR), ultraviolet spectroscopy (UV), Fourier transform-infrared (FT-IR), and matrix-assisted laser desorption ionization time-of-flight mass spectrometry (MALDI-TOF MS) in detail. The arm number and arm length of polystyrene (PS) and poly(tBA) (PAA) in the star polymers were derived from GPC and MALDI-TOF MS after the cleavage of their ester bond linked to the HPG core. It was found that the initiation efficiency for ATRP of the first St was very high (nearly to 100%) but only when the arm number of PS was less than 66 and the molecular weight (MW) of PS was lower than 1 800 Da, then high initiation efficiency for RAFT of the second tBA could reach to 93%.

## Introduction

Although multiarm star polymers have been known since the late 1940s,<sup>1</sup> only recently did they become synthetically available.<sup>2</sup> The progress was primarily due to recent advances in radical polymerization and synthetic strategies. Instead of living anionic/cationic polymerization, nowadays controlled radical polymerization techniques such as nitroxide-mediated radical polymerization (NMRP),<sup>3</sup> atom transfer radical polymerization (ATRP),<sup>4–8</sup> and reverse addition–fragmentation chain transfer (RAFT)<sup>9</sup> polymerization are typically employed to synthesize multiarm star polymers with controlled structural and narrow polydispersity (PDI). Two major synthetic strategies began to be widely used for the preparation of multiarm star polymers: (1) the core-first approach,<sup>10–12</sup> living polymerization on the basis of a multifunctional initiator core, and (2) the arm-first approach,<sup>13–15</sup> linking reactions of polymer chains with a small amount of bifunctional vinyl compounds. Among them, the materials obtained by arm-first strategy are usually less defined than those by the core-first strategy because the former afforded the star polymers with a random distribution of arms per macromolecule. In contrast, when the polymerization was performed by the core-first approach using a multifunctional initiator, the star polymers with a predetermined numbers of arms could be obtained. Nevertheless, it is still a challenge for the preparation of multiarm star polymers because of the dramatic increase of radical–radical coupling probability with the increase of the arm number during the polymerization and the tedious manipulation of purification.<sup>16</sup>

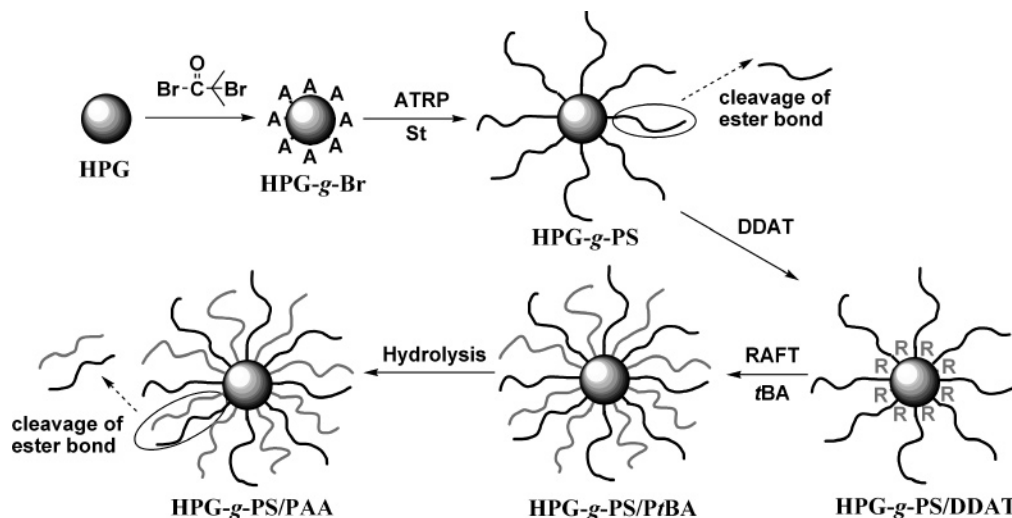
Dendrimers and hyperbranched polymers are attractive precursors of macroinitiators for the reparation of multiarm star polymers by the core-first strategy. However the hyperbranched

polymers prepared by one step from AB<sub>2</sub> type molecules were more widely used because of the complicated preparation procedure of the dendrimers. Among them, hyperbranched polyglycerol (HPG) with narrow polydispersity, which is obtained via ring-opening multibranching polymerization (ROM-BP) under slow addition of the monomer,<sup>17–19</sup> is one of the most promising cores for multiarm star polymers.<sup>20–28</sup>

In the multiarm star polymers, the star polymers with chemically different mixed-arm were very significant polymers due to their unique architectures. They showed some interesting properties in the solid state as well as in solution<sup>29–31</sup> and enable potential applications, including use as drug carriers,<sup>32</sup> membrane formation,<sup>33</sup> and paint additive applications.<sup>34</sup> Till now, mixed-arm star polymers with several arms (arm number < 10) have been reported in a pack of papers mostly with the arm-first strategy using living anionic/cationic polymerization.<sup>2,31,35</sup> For preparation of the polymers with a larger number of arms (arm numbers > 10), the publications are limited because of the difficulty of synthesis. Matyjaszewski et al.<sup>36</sup> reported the synthesis of mixed-arm star polymers (polyMMA)<sub>88</sub>×47–polySS<sub>18</sub>×47–(polyBA)<sub>389</sub>×9 via ATRP by combination of the “arm-first” and “core-first” methods. Qiao et al.<sup>37</sup> prepared PEGDMA–PMMA<sub>14.8</sub>/PCL<sub>38.3</sub> using the “arm-first” method. One drawback of the combination of the “arm-first” and “core-first” methods is the unknown efficiency of the chain extension reaction with the second monomer since not all of the initiation sites in the core would be accessible due to the high cross-linking density in the core and the steric hindrance created by the first kind of arms. On the other hand, although the “arm-first” approach could be conducted by simply cross-linking two different polymeric macroinitiators (polyA and polyB) simultaneously using small difunctional molecule, these two macroinitiators should have the similar reactivity, otherwise it was impossible to obtain the star polymer which contains both polyA

\* Corresponding author. Junlian Huang; e-mail: jlhuang@fudan.edu.cn.

Scheme 1. Synthetic Procedure of HPG-g-PS/PtBA(PAA) Mixed-Arm Star Polymers and Their Cleavage by Sodium Hydroxide (A Represents the Br Groups for ATRP and R Represents the DDAT Groups for RAFT)



and polyB arms. One important challenge in the synthesis of mixed-arm star polymers using the “core first” strategy is to determine the initiation efficiency of the polymerization for the second monomer, i.e., the percentage of initiation sites that actually initiated the polymerization of the second monomer. It could be expected that not all of the initiation sites would be efficiently activated in the polymerization of the second monomer because the core was enwrapped by existing arms formed by the first monomers. Thus, evaluation of initiation efficiency for the polymerization of the second monomers would be a significant challenge because the presence of the first multiarms hinders the following accurate analysis of star polymers using nuclear magnetic resonance spectroscopy (NMR) or gel permeation chromatography (GPC).

The strategy proposed here is to break the ester bond between the core and the arms first, the cleaved linear polymer chains could be measured by standard techniques, and then it would be possible to determine the initiation efficiency in the second polymerization.

In this article, the synthesis of mixed-arm star polymer HPG-g-PS/PtBA and HPG-g-PS/PAA was described by the combination of ATRP and RAFT using the “core first” strategy. The initiation efficiency of the RAFT agents for the polymerization of tBA was evaluated by matrix-assisted laser desorption-time-of-flight (MALDI-TOF) and NMR after the linear arms were cleaved from the mixed-arm star polymers in the presence of sodium hydroxide. (Scheme 1)

## Experimental Section

**Materials.** 1,1,1-Tris(hydroxymethyl)propane, glycidol, 2-bromoisobutyryl bromide, CuBr, and 2,2'-bipyridyl (BPY) were purchased from Aldrich and used as received. Styrene (St) and *tert*-butyl acrylate (tBA) were dried with CaH<sub>2</sub> and distilled under reduced pressure before use. 2, 2-Azobisisobutyronitrile (AIBN) was recrystallized twice in methanol. Other common reagents and solvents were purchased from Sinopharm Chemical Reagent Co., Ltd (SRC) and purified by standard procedure. Hyperbranched polyglycerol (HPG1,  $M_n = 44\,500$  g/mol,  $M_w/M_n = 1.33$ , 600 hydroxyl groups and HPG2,  $M_n = 30\,000$  g/mol,  $M_w/M_n = 1.27$ , 400 hydroxyl groups) and *S*-1-dodecyl-*S'*-( $\alpha,\alpha'$ -dimethyl- $\alpha''$ -acetic acid)trithiocarbonate (DDAT) were synthesized according to refs 18 and 38, respectively.

**Esterification of HPG with 2-Bromoisobutyryl Bromide.** The synthesis of HPG2-g-PS/PtBA(PAA)1 is presented as an example for all of the synthesis section. An amount of 3.0 g (0.1 mmol) of

HPG2 (40 mmol hydroxyl groups) was dried by azeotropic distillation with toluene and then dissolved in 100 mL of anhydrous pyridine, to which 0.75 mL (6 mmol) of 2-bromoisobutyrylbromide was added dropwise at 0 °C over 30 min under vigorous stirring. The reaction was allowed to proceed overnight. A large part of pyridine was distilled under reduced pressure first and then distilled with toluene; the residue was washed with cyclohexane three times and dialyzed against deionized water to ensure all the impurities were moved out. After removal of the water (vacuum, 50 °C), transparent and viscous HPG-g-Br with a pale yellow color was obtained. The percentage of esterification is 16.5%, which means 66 hydroxyl groups on one HPG2 (400 hydroxyl groups) were esterified. <sup>1</sup>H NMR (CD<sub>3</sub>OD)  $\delta$  (ppm): 0.92 (s, 3H, CH<sub>3</sub>-CH<sub>2</sub>- of TMP); 1.45 (s, 2H, CH<sub>3</sub>-CH<sub>2</sub> of TMP); 1.96 (s, 6H, -C(CH<sub>3</sub>)<sub>2</sub>-Br); 3.40–4.00 (m, 5H, CH, CH<sub>2</sub> of HPG); 4.87 (s, OH); 4.24, 4.39, 4.53, 5.17, 5.28 (m, 4H, Br-C(CH<sub>3</sub>)<sub>2</sub>-COO-CH<sub>2</sub>-, Br-C(CH<sub>3</sub>)<sub>2</sub>-COO-CH-). FT-IR (cm<sup>-1</sup>): 1076 (-C-O-C-), 1731 (-COO-), 3200–3500 (-OH).

**Synthesis of Multiarm Star Polymer HPG-g-PS.** An amount of 0.5 g (0.013 mmol, i.e., 0.8 mmol Br atoms) of HPG2-g-Br1, 0.11 g (0.8 mmol) of CuBr, 0.12 g (0.8 mmol) of BPY, and 30 mL (0.26 mol) of styrene were placed in an ampule and freeze-pump-thaw degassed three times. The polymerization was started by immersing the flask into an oil bath at 90 °C. After 5.5 h, the ampule was quenched in liquid nitrogen and exposed to the air, then the unreacted styrene was evaporated and the residue was diluted with CHCl<sub>3</sub>, and the upper solution was collected after centrifuge; the product was precipitated thrice by dissolution/precipitation with methylene chloride/ethanol, and a white powder HPG2-g-PS1 was obtained and dried in vacuo at 40 °C for 24 h. <sup>1</sup>H NMR (CDCl<sub>3</sub>)  $\delta$  (ppm): 0.70–0.95 (s, 6H, -C(CH<sub>3</sub>)<sub>2</sub>-PS); 1.20–2.20 (m, 3H, -CH<sub>2</sub>CH- of PS); 2.80–4.05 (m, 5H, CH, CH<sub>2</sub> of HPG); 4.35–4.65 (d, 1H, CH<sub>2</sub>-CH(Ph)-Br); 6.30–7.30 (m, 5H, -C<sub>6</sub>H<sub>5</sub> of PS). FT-IR (cm<sup>-1</sup>): 1126 (-C-O-C-), 1452, 1492, 1583, 1601 (-C-C-(aromatic ring)) 1731 (-COO-), 3200–3500 (-OH). GPC: MW (hydrodynamic volume), 42 500 Da; PDI = 1.17.

**Cleavage of HPG-g-PS.** An amount of 0.3 g HPG2-g-PS1 was dissolved in 50 mL of tetrahydrofuran (THF), to which 10 mL of KOH solution (1 M in ethanol) was added, and the mixture was refluxed for 72 h. After evaporation to dryness, the polymer was dissolved in CH<sub>2</sub>Cl<sub>2</sub> and by dissolution/precipitation with methylene chloride/ethanol, the PS homopolymer was dried at 50 °C for 24 h. GPC:  $M_n$ , 1 800 Da; PDI = 1.23.

**Esterification of HPG-g-PS with DDAT.** An amount of 1.6 g (0.01 mmol) of HPG2-g-PS1 was dried by azeotropic distillation with toluene, then dissolved in 50 mL of anhydrous and degassed CH<sub>2</sub>Cl<sub>2</sub>, 0.21 g (0.6 mmol) of DDAT, 0.07 g (0.6 mmol) of DMAP, and 0.25 g (1.2 mmol) of DCC were added successively under

Table 1. Preparation of HPG and HPG-g-Br

expt	HPG				HPG-g-Br				
	$M_n^a$	PDI <sup>b</sup>	$N_{OH}^a$	p-OH/s-OH <sup>d</sup>	$N_{Br}^c$	Br (%) <sup>c</sup>	$M_n^c$	$C_{p-OH}^e$ (%)	$C_{s-OH}^f$ (%)
HPG1-g-Br1	44 500	1.33	600	5:7	60	10.0	53 500	18.5	3.9
HPG1-g-Br2	44 500	1.33	600	5:7	110	18.3	61 000	32.1	8.5
HPG2-g-Br1	30 000	1.27	400	7:10	66	16.5	40 000	26.6	8.3
HPG2-g-Br2	30 000	1.27	400	7:10	120	30.0	48 000	51.6	14.8
HPG2-g-Br3	30 000	1.27	400	7:10	210	52.5	61 500	84.8	29.8

<sup>a</sup>  $M_n$  and the number of hydroxyl groups of HPG were measured by  $^{13}C$  NMR. <sup>b</sup> Polydispersity of HPG was measured by GPC using PEO as standard, performed in 0.1 M NaNO<sub>3</sub> aqueous solution. <sup>c</sup> The number and the percentage of Br on one HPG-g-Br and the  $M_n$  of HPG-g-Br were measured by  $^1H$  NMR. <sup>d</sup> The proportion of p (primary) hydroxyl groups and s (secondary) hydroxyl groups on one HPG molecule. <sup>e</sup> The percentage of esterified p (primary) hydroxyl groups by total primary hydroxyl groups on one HPG molecule. <sup>f</sup> The percentage of esterified s (secondary) hydroxyl groups by total secondary hydroxyl groups on one HPG molecule.

0 °C. After stirring for 10 h, the solution was concentrated to 1/3 of its original volume and precipitated in cold ethanol. The filtered product, named as HPG2-g-PS1/DDAT, was dried in vacuo at 40 °C for 24 h. A pale yellow powder was obtained.  $^1H$  NMR (CDCl<sub>3</sub>)  $\delta$  (ppm): 0.70–0.95 (m, 9H,  $-C(CH_3)_2-PS$ ,  $-CH_2-(CH_2)_{10}-CH_3$ ); 1.20–2.20 (m, 3H,  $-CH_2CH-$  of PS); 1.25, 1.31, 1.37, 1.41 (m, 20H,  $-CH_2-(CH_2)_{10}-CH_3$ ); 1.67 (s, 6H,  $-C(CH_3)_2-SC(=S)S-(CH_2)_{11}-CH_3$ ); 3.49 (t, 2H,  $-CH_2-(CH_2)_{10}-CH_3$ ); 2.80–4.05 (m, 5H, CH, CH<sub>2</sub> of HPG); 4.35–4.65 (d, 1H, CH<sub>2</sub>-CH(Ph)-Br); 6.30–7.30 (m, 5H,  $-C_6H_5$  of PS).

**Synthesis of HPG-g-PS/PtBA Mixed-Arm Star Polymer.** An amount of 1.0 g (0.006 mmol, containing 0.4 mmol DDAT groups) of HPG2-g-PS1/DDAT, 6.5 mg (0.04 mmol) of AIBN, 8 mL of tBA, and 2 mL of toluene were placed in an ampule and freeze-pump-thaw degassed three times. The polymerization was started by immersing the flask into an oil bath at 80 °C. After 15 h, the ampule was quenched in liquid nitrogen and exposed to the air; the reaction mixture was concentrated to 1/3 of its original volume and then precipitated in a mixed solution of ethanol and water (v/v: 1:1). The crude product HPG2-g-PS/PtBA1 was purified by dissolution/precipitation with methylene chloride/ethanol/water = 1:1 twice and dried in vacuo at 40 °C for 24 h. A yellow rubberlike powder was obtained.  $^1H$  NMR (CDCl<sub>3</sub>)  $\delta$  (ppm): 0.70–0.95 (m, 9H,  $-C(CH_3)_2-PS$ ,  $-CH_2-(CH_2)_{10}-CH_3$ ); 1.14 (s, 6H,  $-C(CH_3)_2-PtBA$ ); 1.20–2.20 (m, 25H,  $-CH_2CH-$  of PS,  $-CH_2CH-$  of PtBA,  $-CH_2-(CH_2)_{10}-CH_3$ ); 1.50 (s, 9H,  $-C(CH_3)_3$ ); 2.22 (s, 1H,  $-CH_2-CH-$  of tBA); 2.80–4.05 (m, 5H, CH, CH<sub>2</sub> of HPG); 4.35–4.65 (d, 1H, CH<sub>2</sub>-CH(Ph)-Br); 6.30–7.30 (m, 5H,  $-C_6H_5$  of PS). FT-IR (cm<sup>-1</sup>): 1126 ( $-C-O-C-$ ); 1451, 1478, 1494, 1598 ( $-C-C-$  (aromatic ring)); 1727 ( $-COO-$ ); 3200–3500 ( $-OH$ ). GPC: MW (hydrodynamic volume), 44 000 Da; PDI = 1.19.

**Preparation of HPG-g-PS/PAA Mixed-Arm Star Polymer.** An amount of 1.0 g of HPG2-g-PS/PtBA1 and 3.8 mL (0.02 mol) of trifluoroacetic acid (TFA) was dissolved in 50 mL of CH<sub>2</sub>Cl<sub>2</sub>, stirred for 36 h at room temperature. All volatiles were removed under reduced pressure, and the pale gray residue was dried at 40 °C under vacuum for 24 h.  $^1H$  NMR (DMSO-*d*<sub>6</sub>)  $\delta$  (ppm): 0.70–0.95 (m, 9H,  $-C(CH_3)_2-PS$ ,  $-CH_2-(CH_2)_{10}-CH_3$ ); 1.14 (s, 6H,  $-C(CH_3)_2-PAA$ ); 1.20–2.20 (m, 25H,  $-CH_2CH-$  of PS,  $-CH_2CH-$  of PAA,  $-CH_2-(CH_2)_{10}-CH_3$ ); 2.22 (s, 1H,  $-CH_2-CH-$  of PAA); 2.80–5.00 (m, 6H, CH, CH<sub>2</sub> of HPG, CH<sub>2</sub>-CH(Ph)-Br, H<sub>2</sub>O); 6.30–7.30 (m, 5H,  $-C_6H_5$  of PS). FT-IR (cm<sup>-1</sup>): 1126 ( $-C-O-C-$ ); 1451, 1494, 1600 ( $-C-C-$  (aromatic ring)); 1715 ( $-COO-$ ); 2400–3400 ( $-COOH$ ).

**Cleavage of HPG-g-PS/PAA.** An amount of 0.5 g of HPG2-g-PS/PAA1 was dissolved in 30 mL of THF, 10 mL of KOH solution (1 M in ethanol) was added, and the mixture was refluxed for 72 h. After neutralization with 5% HCl and evaporation to dryness, the polymer was redissolved in ethanol. The insoluble PS precipitate was removed by filtration, and the PAA solution was purified by dialysis against water for 72 h to completely remove impurities. MALDI-TOF MS:  $M_n$  = 1 850 Da.

**Measurements.** The number average molecular weight (hydrodynamic volume) and polydispersity index  $M_w/M_n$  were measured by gel permeation chromatography (GPC). For the HPG, GPC was performed in a 0.1 M NaNO<sub>3</sub> aqueous solution at 40 °C with an

elution rate of 0.5 mL/min on an Agilent 1100 with a G1310A pump, a G1362A refractive index detector, and a G1315A diode-array detector, and PEO standard samples were used for calibration. GPC traces of the rest of the polymers were performed in tetrahydrofuran at 35 °C with an elution rate of 1.0 mL/min on an Agilent 1100 with a G1310A pump, a G1362A refractive index detector, and a G1314A variable wavelength detector, and polystyrene standard samples were used for calibration.  $^1H$  NMR and  $^{13}C$  NMR spectra were obtained on a DMX 500 MHz spectrometer using tetramethylsilane (TMS) as the internal standard and CDCl<sub>3</sub>, CD<sub>3</sub>OD, and DMSO-*d*<sub>6</sub> as the solvents. Fourier transform infrared (FT-IR) spectra were recorded on a Magna 550 FT-IR instrument; the polymer samples were dissolved in dry dichloromethane or methanol and then cast onto a NaCl disk to form the film by the evaporation of the solvent under the infrared lamp. The MALDI-TOF MS measurement was performed using a Perspective Biosystem Voyager-DE STR MALDI-TOF mass spectrometer (PE Applied Biosystems, Framingham, MA) equipped with a nitrogen laser emitting at 337 nm with a 3 ns pulse width and in the negative ion mode. The spectra were recorded in reflectron mode. The matrix solution of dithranol (20 mg/mL) and polymer (10 mg/mL) were mixed in the ratio of matrix/polymer = 5:1, and 0.8  $\mu$ L of the mixed solution was deposited on the sample holder (well-plate).

## Results and Discussion

Considering that the activation of an ATRP initiator by a metal complex is a bimolecular process and the free radicals in RAFT are generated by thermal decomposition, a unimolecular process, ATRP of PS, was conducted first. Otherwise, after RAFT of the first monomer, ATRP of the second monomer is very difficult to be carried out due to possible steric hindrance from the existing polymer chains for a bimolecular process. Generally, three steps were needed to synthesize HPG-g-PS/PtBA mixed-arm star polymers using sequential ATRP and RAFT polymerization via the “core-first” method. First, the hyperbranched ATRP macroinitiators employed were prepared on the basis of well-defined HPG by esterification with 2-bromoisobutryl bromide. After polymerization with styrene (St), HPG-g-PS was further converted into macro-RAFT agents by esterification with *S*-1-dodecyl-*S'*-( $\alpha,\alpha'$ -dimethyl- $\alpha''$ -acetic acid)trithiocarbonate (DDAT), then HPG-g-PS/PtBA was obtained by RAFT polymerization of *tert*-butyl acrylate (tBA).

**Esterification of HPG with 2-Bromoisobutryl Bromide.** Hyperbranched polyglycerol samples HPG1 ( $M_n$  = 44 500 g/mol,  $M_w/M_n$  = 1.33, 600 hydroxyl groups, with 250 primary hydroxyl groups) and HPG2 ( $M_n$  = 30 000 g/mol,  $M_w/M_n$  = 1.27, 400 hydroxyl groups, with 165 primary hydroxyl groups) were prepared by anionic polymerization of glycidol using trimethylolpropane (TMP) as an initiator according to previously published references.<sup>17,18</sup> On HPG, there are two kinds of OH groups, primary and secondary, and the ratio between them could be determined by  $^{13}C$  NMR<sup>17,18</sup> (see Table 1); the value is about 5:7 for HPG1 and 7:10 for HPG2 (primary OH number/



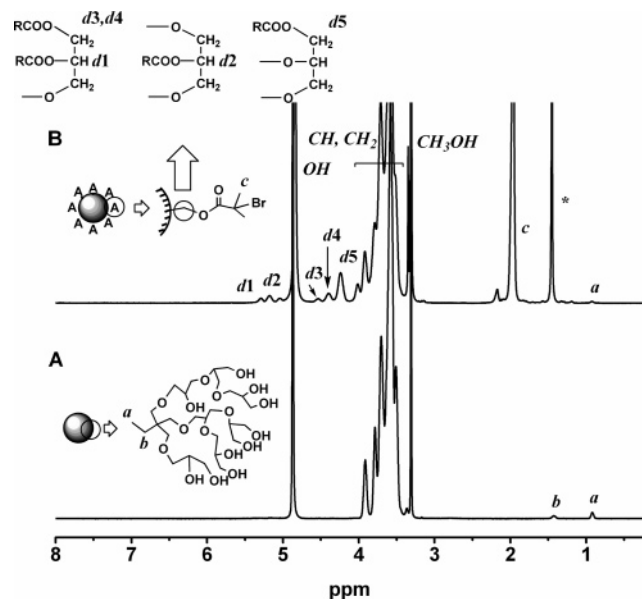


**Figure 1.**  $^1\text{H}$  NMR spectra of (A) HPG and (B) HPG-g-Br (solvent,  $\text{CD}_3\text{OD}$ ).

secondary OH number). Subsequently, the hydroxyl groups of HPG were esterified by 2-bromoisobutyrylbromide to generate macroinitiators HPG-g-Br for ATRP. Five macroinitiators with an average of 60 and 110 initiation sites for HPG1 and 66, 120, and 210 initiation sites for HPG2 were prepared and shown in Table 1. Figure 1 is the  $^1\text{H}$  NMR spectra of HPG before and after reaction with 2-bromoisobutyrylbromide. Comparing with Figure 1A for the HPG scaffold, the original five resonances observed in the range of 3.4–4.1 ppm for methylene and methine were moved to 4.1–5.5 ppm (d) (d1–d5) in Figure 1B, d1 and d2 are the resonance for the protons of the methine group of the esterified secondary hydroxyl groups; d3–d5 are the resonance for the protons of the methylene group of the esterified primary hydroxyl groups.<sup>22</sup> It was found that the primary hydroxyl groups are much more reactive than the secondary hydroxyl groups although there are more secondary hydroxyl groups on the HPG molecules as Table 1 shows. The appearance of the resonances at 1.95 ppm (c) for the protons of the methyl groups close to the Br atom also proved the successful reaction. Thus, the Br number ( $N_{\text{Br}}$ ) of HPG2-g-Br1 can be calculated by following two ways:

$$N_{\text{Br}} = \frac{A_c/6}{A_{3.1-4.4}/5} \times 400 \quad (1)$$

$$N_{\text{Br}} = \frac{A_{d1} + A_{d2} + (A_{d3} + A_{d4})/2 + A_{d5}/2}{A_{3.1-4.4}/5} \times 400 \quad (2)$$

where  $A_c$  and  $A_{3.1-4.4}$  are the integral areas of the protons on the methyl groups close to the Br atom at 1.95 ppm (c) and the HPG scaffold hydrogens (3.4–4.1 ppm), respectively.  $A_{d1}$ – $A_{d5}$  are the five peaks in the region 4.1–5.5 ppm (d) which are attributed to methylene and methine protons connected to the ester bond after esterification. Both results are co-incident,  $N_{\text{Br}}$  was 66 by eq 1 and 64 by equation 2.

Figure 2 is the FT-IR analysis of HPG (Figure 2A) and HPG-g-Br (Figure 2B), and the appearance of a characteristic ester group at  $1731\text{ cm}^{-1}$  compared to the HPG (Figure 2A) supported the synthesis of HPG-g-Br. As it is well-known, the purity of the ATRP macroinitiators may exert a great effect on the polymerization.<sup>16</sup> In the ATRP macroinitiators, there are two

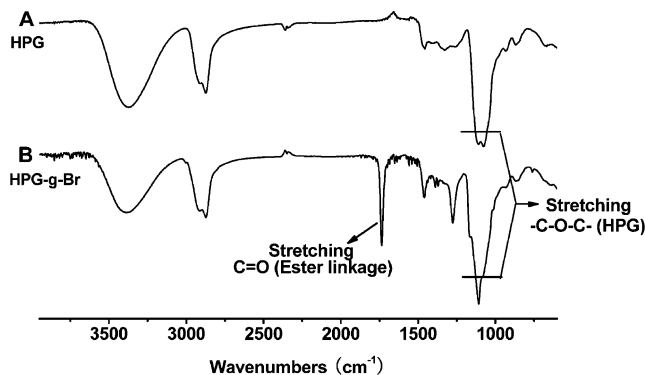


**Figure 2.** FT-IR spectra of (A) HPG and (B) HPG-g-Br.

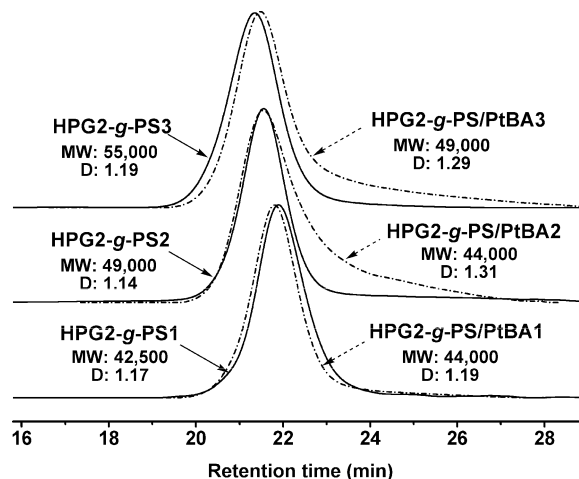


**Figure 3.** GPC curves of HPG-g-PS and HPG-g-PS/PtBA.

major impurities: small ATRP initiators from 2-bromoisobutyryl bromide and pyridine salts from the pyridine solution. In this work, cyclohexane was first used to wash away small molecular ATRP initiators, then for HPG1-g-Br1 and HPG2-g-Br1 which are hydrophilic, the pyridine salts were removed by dialysis against water. For HPG1-g-Br2, HPG2-g-Br2, and HPG2-g-Br3 which are hydrophobic, the pyridine salts were removed by washing with water. After purification, we cannot find any trace of pyridine salts and small molecular ATRP initiators through UV and  $^1\text{H}$  NMR spectra, which proved that the purification was successful.

#### Synthesis of Multiarm Star Polymer HPG-g-PS by ATRP.

ATRP of St using the HPG-based macroinitiator could only be conducted in limited conversions (<35%), since higher conversion may cause the gel formation.<sup>22</sup> This result was in agreement with previous observations by Gnanou et al.<sup>10</sup> and was attributed to the coupling reactions between radicals. To suppress this process, in our system, the styrene monomer conversion was controlled below 20%. It was observed that the MW (hydrodynamic volume) of stars, estimated from GPC with linear polystyrene standards, were smaller than the values theoretically predicted due to the smaller hydrodynamic volume of the star polymers than that of the linear chains, so the MW of HPG-g-PS obtained from GPC was unreliable. Figure 3 shows the GPC curves of HPG-g-PS which proves that the ATRP processes are controllable but the  $M_n$ 's of HPG-g-PS are much smaller compared to the real  $M_n$ 's. On the other hand, in the star polymers, the HPG core were wrapped by the PS chains, so the integration of the proton peak area of HPG and part of the PS chain close to the core in NMR were not very accurate; thus, the methine and methylene protons from the HPG core showed a weak and broad peak in the  $^1\text{H}$  NMR spectrum due to the partial immobilization of the HPG in the star core, and

Table 2. Preparation of HPG-g-PS

expt	$N_{\text{Br}}$	conversion(%)	HPG-g-PS					PS		
			$M_n^a$	PDI <sup>a</sup>	$M_n$ (calcn 1) <sup>b</sup>	$M_n$ (calcn 2) <sup>c</sup>	$M_n$ (calcn 2)/ $M_n$	$M_n^a$	$M_n^d$	PDI <sup>a</sup>
HPG1-g-PS1	60	7.9	47 000	1.21	284 000	227 000	4.83	2 900	3 050	1.20
HPG1-g-PS2	110	19.7	56 800	1.26	716 000	500 000	8.80	4 000	3 960	1.19
HPG2-g-PS1	66	9.2	42 500	1.17	241 000	160 000	3.76	1 800	1 920	1.23
HPG2-g-PS2	120	16.3	49 000	1.14	475 000	310 000	6.32	2 200	2 480	1.16
HPG2-g-PS3	210	18.9	55 000	1.19	695 000	690 000	12.54	3 000	3 200	1.31

<sup>a</sup> Molecular weight (hydrodynamic volume) and PDI of HPG-g-PS and PS after cleavage measured by GPC using PS as standard and THF as eluent.

<sup>b</sup> Molecular weight of HPG-g-PS calculated by St monomer conversion using eq 3. <sup>c</sup>  $M_n$  of HPG-g-PS calculated by the molecular weight ( $M_n$ ) of PS chains after cleavage using eq 4. <sup>d</sup>  $M_n$  of PS after cleavage measured by MALDI-TOF.

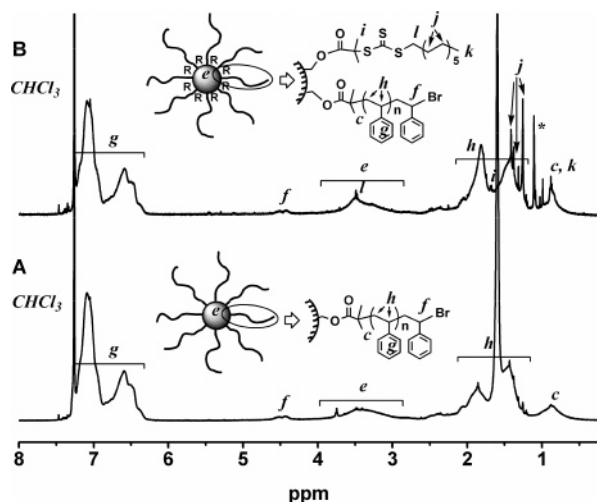


Figure 4. <sup>1</sup>H NMR spectra of (A) HPG-g-PS and (B) HPG-g-PS/DDAT (solvent, CDCl<sub>3</sub>).

this deviation for the measurement of molecular weight is inevitable for the NMR analysis of star polymers.<sup>16</sup> In this article, two methods were used to determine the  $M_n$  of HPG-g-PS: derived by St monomer conversion ( $M_n$  calcn 1) and by  $M_n$  of linear PS chains cleaved from HPG-g-PS ( $M_n$  calcn 2) (see Table 2).

$$M_n(\text{calcn 1}) = \frac{(\text{St}_{\text{conversion}})(30)(0.909)}{0.5} (M_n(\text{HPG-g-Br}) + M_n(\text{HPG-g-Br})) \quad (3)$$

$$M_n(\text{calcn 2}) = ((M_n(\text{PS}))(N_{\text{Br}})) + M_n(\text{HPG-g-Br}) \quad (4)$$

where in  $M_n$  (calcn 1),  $\text{St}_{\text{conversion}}$  is the monomer conversion of St, 30 (in mL) is the used St volume in ATRP, 0.909 is the density of St, 0.5 (in g) is the HPG-g-Br used weight in ATRP for HPG-g-PS,  $M_n$  (HPG-g-Br) is the  $M_n$  of HPG-g-Br from <sup>1</sup>H NMR. In eq 4,  $M_n$  (PS) is the  $M_n$  of PS after cleavage from HPG-g-PS by GPC,  $N_{\text{Br}}$  is the number of Br groups on HPG-g-Br, and  $M_n$  (HPG-g-Br) is the  $M_n$  of HPG-g-Br from <sup>1</sup>H NMR. Both of the results were agreeable as Table 2 showed.

The values of  $M_n$  (calcn 2) were selected for the following reaction. It was found that the more arms of the star polymers, the higher the compact structure value  $M_n$  (calcn 2)/ $M_n$  (GPC).<sup>36</sup> As Table 2 showed that the star polymer HPG2-g-PS3 with the most arms (arm number = 210) has the highest compact structure value 12.54, that means HPG2-g-PS3 was more compact than any of the other samples. Comparing the <sup>1</sup>H NMR spectra Figure 1B and Figure 4A, after polymerization (Figure 4A) the signals at 1.27–2.25 ppm (h) and 6.27–7.22 ppm (g) for St units appear; the peak at 1.94 ppm (c) for methyl groups close to the Br atom is shifted to higher field (0.7–1.0 ppm) because of the change of the carbon–bromine bond to the

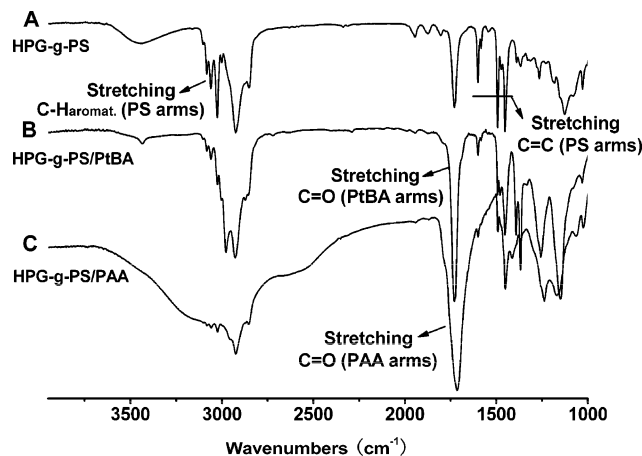


Figure 5. FT-IR spectra of (A) HPG-g-PS and (B) HPG-g-PS/PtBA, and (C) HPG-g-PS/PAA.

carbon–carbon bond of the tertiary carbon; the appearance of the new peak at 4.35–4.65 ppm (f) is corresponding to the methine proton on (CH<sub>2</sub>–CH(Ph)–Br).

These changes could prove that the ATRP was successful, and all the initiating sites on HPG were served in ATRP. This was also confirmed by Holger Frey et al. in their previous work.<sup>22,27,28</sup> The FT-IR spectrum of HPG-g-PS is shown in Figure 5A, and the characteristic bands of PS blocks C=C<sub>aromatic</sub> stretching at 1450–1601 cm<sup>−1</sup> and C–H<sub>aromatic</sub> stretching at 3020–3100 cm<sup>−1</sup> indicate the successful polymerization of the St monomer.

**Esterification of HPG-g-PS with DDAT.** DDAT is a good chain transfer agent with extremely high-chain transfer efficiency. It can control the bulk or solution polymerizations of alkyl acrylates, acrylic acid, and styrene very well.<sup>38</sup> The number of DDAT groups ( $N_{\text{DDAT}}$ ) on one HPG core was measured by <sup>1</sup>H NMR, Parts A and B of Figure 4 showed the <sup>1</sup>H NMR spectra of HPG-g-PS and HPG-g-PS/DDAT, respectively. In comparison with the <sup>1</sup>H NMR spectra before and after the reaction of HPG-g-PS with DDAT, the peaks at 1.25, 1.31, 1.38, and 1.41 ppm (j) attributed to the protons of the methylene of DDAT appeared in HPG-g-PS/DDAT, and the resonance of 0.88 ppm (k) was increased due to the attribution of the methyl group at the DDAT end. The exact value of  $N_{\text{DDAT}}$  was calculated by following formula:

$$N_{\text{DDAT}} = N_{\text{Br}} \frac{(A_{\text{g(B)}}A_{\text{c,k(B)}}) - (A_{\text{g(A)}}A_{\text{c(A)}})}{3A_{\text{f(B)}}} \quad (5)$$

where  $A_{\text{c,k(B)}}$ ,  $A_{\text{g(B)}}$ , and  $A_{\text{f(B)}}$  are the integral areas of 0.88 ppm (methyl group at the DDAT end and methyl groups close to the ester bond on PS arms), 6.30–7.30 ppm (aromatic ring of PS), and 4.35–4.65 ppm (methine close to Br on PS arms) on HPG-g-PS/DDAT;  $A_{\text{g(A)}}$  and  $A_{\text{c(A)}}$  are the integral areas of 0.88 ppm (methyl groups close to the ester bond on PS arms) and

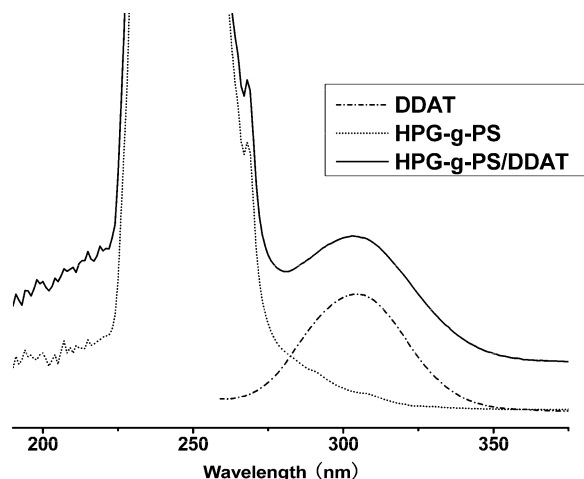


**Figure 6.** UV spectra of DDAT, HPG-g-PS, and HPG-g-PS/DDAT (concentration for HPG-g-PS/DDAT, HPG-g-PS, and DDAT in  $\text{CH}_2\text{Cl}_2$  solution was  $1 \times 10^{-6}$  mol/L, respectively).

6.30–7.30 ppm (aromatic ring of PS) on HPG-g-PS, and  $N_{\text{Br}}$  is the Br groups on one HPG-g-PS/DDAT molecule.

To guarantee the reliability of the data obtained from  $^1\text{H}$  NMR, UV was used for further confirmation. The maximal absorbance of small molecule DDAT was found at 307 nm, and the molar extinction coefficient ( $\epsilon$ ) was  $1.383 \times 10^4 \text{ L mol}^{-1} \text{ cm}^{-1}$ . The contents of the DDAT groups in HPG-g-PS/DDAT could be derived from the relationship between the used concentration of HPG-g-PS/DDAT and absorbance of DDAT in UV. To make sure that the unreacted DDAT was completely removed, the HPG-g-PS/DDAT samples were washed several times with ethanol until there was no UV absorbance at 307 nm of the collected washing ethanol. Thus, the absorbance at 307 nm could be attributed to the DDAT end groups of HPG-g-PS/DDAT. Figure 6 showed the UV absorption spectra of HPG-g-PS/DDAT, HPG-g-PS, and DDAT. The number of DDAT groups ( $N_{\text{DDAT}}$ ) was calculated with the following equation:

$$N_{\text{DDAT}} = \frac{A}{\epsilon l} \quad (6)$$

where  $A$  is the absorbance of HPG-g-PS/DDAT at 307 nm measured with the UV spectrum and  $l$  is the length of the sample cell (1 cm). The obtained value was listed in Table 3 and was co-incident with the NMR results. The mole ratio of concentration of DDAT and bromine on HPG-g-PS/DDAT was designed as 1:1, and all samples shown in Table 3 were close to 1:1 except HPG2-g-PS/DDAT3 because of its denser Br groups (210) with the remaining 190 hydroxyl groups. Esterification of these remaining hydroxyl groups with DDAT as high as possible was

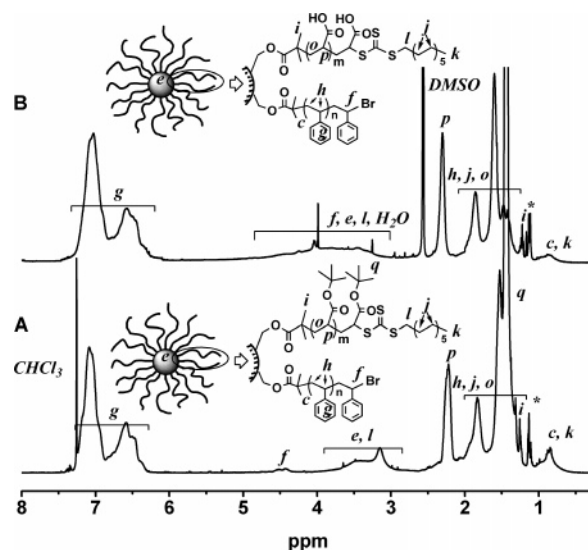


**Figure 7.**  $^1\text{H}$  NMR spectra of (A) HPG-g-PS/PtBA (solvent,  $\text{CDCl}_3$ ) and (B) HPG-g-PS/PAA (solvent,  $\text{DMSO}-d_6$ ).

a challenge for polymer chemists, since the HPG cores were wrapped by existed PS chains to lead to the low esterification of the remaining hydroxyl groups.

**Synthesis of HPG-g-PS/PtBA(PAA) Mixed-Arm Star Polymer by RAFT.** To suppress the coupling reactions between radicals, monomer (tBA) conversion in the RAFT polymerization was also controlled below 20%. Figure 7A shows the  $^1\text{H}$  NMR spectra of HPG-g-PS/PtBA. The new peak at 2.22 ppm (p) corresponding to the methine proton on the main chain of the tBA units appears besides the characteristic signals of HPG at 2.80–4.05 ppm (e) and St units at 6.30–7.30 ppm (g). Additionally, the appearance of methyl protons of PtBA at 1.50 ppm (q) could also be observed. The FT-IR spectrum of HPG-g-PS/PtBA was shown in Figure 5B, except the typical absorption peaks of PS arms at  $1450\text{--}1600 \text{ cm}^{-1}$  for  $\text{C}=\text{C}_{\text{aromat}}$  stretching and at  $3020\text{--}3100 \text{ cm}^{-1}$  for  $\text{C}-\text{H}_{\text{aromat}}$  stretching, the HPG core at  $1126 \text{ cm}^{-1}$  for  $\text{C}-\text{O}-\text{C}$  stretching and a strong peak at  $1727 \text{ cm}^{-1}$  of the  $\text{C}=\text{O}$  stretching band for PtBA arms were observed. It confirmed that the chemical components of the desired HPG-g-PS/PtBA were synthesized successfully. After hydrolysis of the PtBA arms of HPG-g-PA/PtBA in the presence trifluoroacetic acid, the amphiphilic mixed-arm star polymer HPG-g-PA/PAA was obtained. Figure 7B shows the  $^1\text{H}$  NMR spectra of HPG-g-PS/PAA. Compared to Figure 7A, the peak strength at 1.50 ppm assigned to the methyl protons of the tBA units which are overlapped with the methylene protons of the St units decreased, which means the ester groups of the tBA units were hydrolyzed successfully. FT-IR analysis also supported the presence of the acid groups shown in Figure

**Table 3.** Preparation of HPG-g-PS/DDAT, HPG-g-PS/PtBA, and HPG-g-PS/PAA

expt	HPG-g-PS/DDAT				PAA $M_n^d$	HPG-g-PS/PAA $M_n^e$	HPG-g-PS/PtBA		
	$N_{\text{DDAT}}^a$	$N_{\text{DDAT}}^b$	EF(%) <sup>b</sup>	EI(%) <sup>c</sup>			$M_n^f$	$M_n^g$	PDI <sup>g</sup>
HPG1-g-PS/PtBA(PAA)1	67	71	11.8	82	1 620	321 000	394 000	41 000	1.23
HPG1-g-PS/PtBA(PAA)2	97	116	19.3	51	1 050	562 000	510 000	43 000	1.27
HPG2-g-PS/PtBA(PAA)1	60	68	17.0	93	1 850	277 000	368 000	44 000	1.19
HPG2-g-PS/PtBA(PAA)2	103	121	30.2	67	1 500	431 600	526 000	44 000	1.31
HPG2-g-PS/PtBA(PAA)3	63	89	22.3	45	760	720 400	744 000	49 000	1.29

<sup>a</sup> The number of DDAT on one HPG-g-PS/DDAT was measured by  $^1\text{H}$  NMR, using eq 5. <sup>b</sup> The number of DDAT on one HPG-g-PS/DDAT was measured by UV, using eq 6, the molar ratio of DDAT and hydroxyl groups on one HPG (EF) was also measured by UV. <sup>c</sup> The initiation efficiency of DDAT (EI) was calculated by eq 9. <sup>d</sup> Molecular weight of PAA was obtained by MALDI-TOF MS. <sup>e</sup>  $M_n$  of HPG-g-PS/PAA was obtained by eq 8. For example, if  $M_n$  of PAA was 117 000, then  $M_n(\text{HPG2-g-PS-PtBA1}) = M_n(\text{HPG2-g-PS}) + ((128/72)M_n(\text{PAAall4})) = 160 000 + ((128/72)117 000) = 368 000$ . <sup>f</sup>  $M_n$  of HPG-g-PS/PtBA was obtained by eq 7. For example, if  $M_n$  of PAA was 117 000, then  $M_n(\text{HPG2-g-PS-PAA1}) = M_n(\text{HPG2-g-PS}) + M_n(\text{PAAall4}) = 160 000 + 117 000 = 277 000$ . <sup>g</sup> Molecular weight (hydrodynamic volume) and PDI of HPG-g-PS/PtBA were measured by GPC using PS as standard and performed in THF.



5C, the broad absorbance of carboxylic acid groups was observed at 2400–3400 cm<sup>-1</sup> and the carbonyl stretch was shifted from 1727 cm<sup>-1</sup> for the ester bond of PtBA to 1715 cm<sup>-1</sup> of the carboxyl group of PAA.

The  $M_n$  (hydrodynamic volume) of HPG-g-PS/PtBA obtained by GPC was close to HPG-g-PS (Figure 3), which means the RAFT polymerization almost does not change its hydrodynamic radius markedly. In order to obtain the reliable molecular weight of HPG-g-PS/PtBA (PAA), the  $M_n$  of HPG-g-PS/PtBA(PAA) could be calculated by following equation from NMR:

$$M_{n(\text{HPG-g-PS/PtBA})} = M_{n(\text{HPG-g-PS})} + \frac{128}{72} M_{n(\text{PAAall})} \quad (7)$$

$$M_{n(\text{HPG-g-PS/PAA})} = M_{n(\text{HPG-g-PS})} + M_{n(\text{PAAall})} \quad (8)$$

where  $M_{n(\text{PAAall})}$  was the  $M_n$  of all the PAA arms on one HPG core and was measured by the  $M_n$  ratio of PS and PAA from NMR after cleavage of the ester bond on HPG-g-PS/PAA. The MW of tBA is 128, and 72 is the MW of AA,  $M_{n(\text{HPG-g-PS})}$  was the  $M_n$  of HPG-g-PS. The data were listed in Table 3.

**Evaluation of the Initiation Efficiency of DDAT Sites in HPG-g-PS/DDAT.** The  $M_n$  of PtBA was derived from the broken PAA chains and the latter was determined by MALDI-TOF MS shown in Table 3. It was found that the  $M_n$  of PAA rapidly decreases with an increase in the number of PS arms and chain length; the  $M_n$  of PtBA obtained in our experiment was less than that of the polymer obtained using DDAT as the small RAFT initiator.<sup>38</sup> This could be explained by the steric hindrance of the existing PS arms, which also would lead to the drop of efficient DDAT functionality. To quantify the initiation efficiency of DDAT sites in the HPG-g-PS/DDAT during the polymerization of tBA, it is significant to know what is the molar ratio of PS and PtBA(PAA) after cleavage ( $M_{n(\text{PAAall})}$ ), thus the DDAT(%)<sub>activated</sub> could be calculated by following equation:

$$\text{DDAT}_{\text{activated}}(\%) = \frac{\frac{M_{n(\text{PAAall})}}{M_{n(\text{PAA})}}}{N_{\text{DDAT}}(\text{UV})} \times 100\% \quad (9)$$

where  $M_{n(\text{PAAall})}$  is calculated by the  $M_n$  ratio of PS and PAA after cleavage of the ester bond on HPG-g-PS/PAA. The  $M_n$  of PAA is determined by MALDI-TOF MS, named  $M_{n(\text{PAA})}$ .  $N_{\text{DDAT}}(\text{UV})$  is the number of DDAT groups on one HPG core determined by UV. As Table 3 showed that in the case of HPG2-g-PS/PtBA(PAA)1, when the number of PS chains and the molecular weight of the PS arm on HPG were less than 66 and 1 800 Da, respectively, the initiation efficiency of DDAT was as high as 93%. When the number of PS chains reached to 120 (HPG2-g-PS/PtBA(PAA)2), only 67% of the total DDAT sites was activated although the arm length of PS did not change much (2 200 Da). It was found that the PS arm length also exerted great effect on the initiation efficiency of DDAT. For example, HPG1-g-PS/PtBA(PAA)1 was the star polymer with 66 PS chains of  $M_n$  2 900 Da, compared with HPG2-g-PS/PtBA(PAA)1 with 60 PS chains of  $M_n$  1 800 Da, and the initiation efficiency of DDAT decreased from 93% to 82%.

## Conclusion

Mixed-arm star polymers, HPG-g-PS/PtBA and HPG-g-PS/PAA were successfully synthesized by sequential ATRP and RAFT using the “core first” method. It was found that the arm length and arm number exert great effect on the structure of

star polymers with mixed-arms. The initiation efficiency of the DDAT in the core of star molecules was evaluated by the linear polymers formed by the cleavage of the ester bond between the core and the mixed-arm in the presence of sodium hydroxide. It was found only if the arm number of PS was less than 66 and the molecular weight of PS was lower than 1 800 Da, then high initiation efficiency (93%) of DDAT could be reached.

**Acknowledgment.** We appreciate the financial support of this research from the Natural Science Foundation of China (Grant No. 20574010).

## References and Notes

- Schaefer, J. R.; Flory, P. J. *J. Am. Chem. Soc.* **1948**, *70*, 2709–2718.
- Teng, J.; Zubarev, E. R. *J. Am. Chem. Soc.* **2003**, *125*, 11840–11841.
- Georges, M. K.; Veregin, R. P. N.; Kazmaier, P. M.; Hamer, G. K. *Macromolecules* **1993**, *26*, 2987–2988.
- Wang, J.; Matyjaszewski, K. *Macromolecules* **1995**, *28*, 7572–7573.
- Wang, J.; Matyjaszewski, K. *J. Am. Chem. Soc.* **1995**, *117*, 5614–5615.
- Wang, J.; Matyjaszewski, K. *Macromolecules* **1995**, *28*, 7901–7910.
- Percec, V.; Barboiu, B. *Macromolecules* **1995**, *28*, (23), 7970–7972.
- Kato, M.; Kamigaito, M.; Sawamoto, M.; Higashimura, T. *Macromolecules* **1995**, *28*, (5), 1721–1723.
- Chieffari, J.; Chong, Y. K. B.; Ercole, F.; Krstina, J.; Jeffery, J.; Le, T. P. T.; Mayadunne, R. T. A.; Meijs, G. F.; Moad, C. L.; Moad, G.; Rizzardo, E.; Thang, S. H. *Macromolecules* **1998**, *31*, 5559–5562.
- Angot, S.; Murthy, K. S.; Taton, D.; Gnanou, Y. *Macromolecules* **1998**, *31*, 7218–7225.
- Ueda, J.; Kamigaito, M.; Sawamoto, M. *Macromolecules* **1998**, *31*, 6762–6768.
- Matyjaszewski, K.; Miller, P. J.; Pyun, J.; Kickelbick, G.; Diamanti, S. *Macromolecules* **1999**, *32*, 6526–6535.
- Zhang, X.; Xia, J.; Matyjaszewski, K. *Macromolecules* **2000**, *33*, 2340–2345.
- Xia, J.; Zhang, X.; Matyjaszewski, K. *Macromolecules* **1999**, *32*, 4482–4484.
- Baek, K.-Y.; Kamigaito, M.; Sawamoto, M. *Macromolecules* **2001**, *34*, 215–221.
- Matyjaszewski, K. *Polym. Int.* **2003**, *52*, 1559–1565.
- Sunder, A.; Hanselmann, R.; Frey, H.; Mulhaupt, R. *Macromolecules* **1999**, *32*, 4240–4246.
- Kautz, H.; Sunder, A.; Frey, H. *Macromol. Symp.* **2001**, *163*, 67–73.
- Kainthan, R. K.; Muliawan, E. B.; Hatzikiriakos, S. G.; Brooks, D. E. *Macromolecules* **2006**, *39*, 7708–7717.
- Sunder, A.; Bauer, T.; Mulhaupt, R.; Frey, H. *Macromolecules* **2000**, *33*, 1330–1337.
- Sunder, A.; Mulhaupt, R.; Frey, H. *Macromolecules* **2000**, *33*, 309–314.
- Maier, S.; Sunder, A.; Frey, H.; Mulhaupt, R. *Macromol. Rapid Commun.* **2000**, *21*, 226–230.
- Burgath, A.; Sunder, A.; Neuner, I.; Mulhaupt, R.; Frey, H. *Macromol. Chem. Phys.* **2000**, *201*, 792–797.
- Knischka, R.; Lutz, P. J.; Sunder, A.; Mulhaupt, R.; Frey, H. *Macromolecules* **2000**, *33*, 315–320.
- Wan, D.; Li, Z.; Huang, J. *J. Polym. Sci., Part A: Polym. Chem.* **2005**, *43*, 5458–5464.
- Wan, D.; Fu, Q.; Huang, J. *J. Polym. Sci., Part A: Polym. Chem.* **2005**, *43*, 5652–5660.
- Chen, Y.; Shen, Z.; Barriau, E.; Kautz, H.; Frey, H. *Biomacromolecules* **2006**, *7*, 919–926.
- Shen, Z.; Chen, Y.; Barriau, E.; Frey, H. *Macromol. Chem. Phys.* **2006**, *207*, 57–64.
- Beyer, F. L.; Gido, S. P.; Poulos, Y.; Avgeropoulos, A.; Hadjichristidis, N. *Macromolecules* **1997**, *30*, 2373–2376.
- Pispas, S.; Poulos, Y.; Hadjichristidis, N. *Macromolecules* **1998**, *31*, 4177–4181.
- Hadjichristidis, N. *J. Polym. Sci., Part A: Polym. Chem.* **1999**, *37*, 857–871.
- Hadjichristidis, N.; Pitsikalis, M.; Pispas, S.; Iatrou, H. *Chem. Rev.* **2001**, *101*, 3747–3792.
- Connal, L. A.; Gurr, P. A.; Qiao, G. G.; Solomon, D. H. *J. Mater. Chem.* **2005**, *15*, 1286–1292.
- Ho, A. K.; Iin, I.; Gurr, P. A.; Mills, M. F.; Qiao, G. G. *Polymer* **2005**, *46*, 6727–6735.
- Heise, A.; Trollsas, M.; Magbitang, T.; Hedrick, J. L.; Frank, C. W.; Miller, R. D. *Macromolecules* **2001**, *34*, 2798–2804.
- Gao, H.; Tsarevsky, N. V.; Matyjaszewski, K. *Macromolecules* **2005**, *38*, 5995–6004.
- Wiltshire, J. T.; Qiao, G. G. *Macromolecules* **2006**, *39*, 9018–9027.
- Lai, J. T.; Filla, D.; Shea, R. *Macromolecules* **2002**, *35*, 6754–6756.